Utilizing a Meso Scale Limited Dome Test to Study the Effect of Strain Rate on the Formability of Commercial Pure Titanium Grade Two Foil

J.-T. Gau*, K. Zhang, Z. Wang
Department of Mechanical Engineering, Northern Illinois University, USA
*Corresponding author. Email: jgau@niu.edu

Abstract

Due to its hexagonal close-packed (HCP) crystal structures and limited slipping systems, commercial pure titanium (CP Ti) has a relatively low ductility at room temperature. In order to understand the effect of strain rate on formability of the as-received tempered CP Ti grade 2 foils with thickness of 38μm, a series of meso-limited dome height (meso-LDH) tests were designed and conducted at three punch speeds (0.01mm/sec, 12m/sec and 17m/sec) without lubricant at room temperature. The forming limit curves of the foil at three different punch speeds were obtained, and can be used right away for product design, process design and development, die design, and simulations etc. As discovered in this experimental study, the reasons why increasing strain rate can improve the formability are: n value increases with increasing strain rate, the temperature of part increases rapidly due to adiabatic effect, and the negative influence of friction can be reduced.

Keywords

Formability; Commercial pure titanium grade 2 foil; Meso-LDH test, Adiabatic effect

1 Introduction

Commercial pure titanium (CP Ti) foils have been widely utilized for producing three-dimensional parts with extremely thin walls because of its lightweight, high specific strength, excellent corrosion resistance and biocompatibility etc. The need of meso and micro scale thin-wall CP Ti parts (thickness ≤50μm) have been increased tremendously due to the trend of miniaturization in many applications such as automotive, aerospace, sensor, medical, electronic, and energy industries etc. It is desired to form parts at room temperature for minimizing energy consumption and to understand the effect of strain rates on forming the extremely thin commercial pure titanium grade 2 (CP Ti Gr2) foils. However, it has a relatively low ductility at room temperature due to its hexagonal close-packed (HCP) crystal structures and limited slipping systems. Therefore, forming titanium and titanium alloys parts at elevated temperatures is widely used for obtaining better formability. For example, Chen and Chiu (2005) examined thermal effect and strain rate effect on formability of commercial pure titanium sheet with thickness of 0.5mm by a

series of tensile tests, v-bend tests, circular cup drawing tests and forming limit tests. For tensile tests, they conducted the tests at 4 different temperatures (room temperature, 100℃, 200℃ , and 300℃) and different strain rates at room temperature ($0.0001s^{-1}$, $0.001s^{-1}$, $0.01s^{-1}$ and $0.1s^{-1}$). From their study, the flow stress curve is getting lower proportionally with increasing of testing temperature, which means that the material is getting easier to be formed at higher forming temperature, but the flow stress curve of commercial pure titanium increases with the increase of strain rates. It can be concluded from their tensile test data that commercial pure titanium exhibits better formability at elevated temperature.

Furthermore, Tsao et al. (2012) also conducted a series of tensile tests on CP Ti (1.6mm) specimens with 10mm gauge length and 6mm gauge width at four different temperatures (623ºK, 673ºK, 723ºK, and 773ºK) and four strain rates ($5.0 \times 10^{-2}s^{-1}, 1.6 \times 10^{-2}s^{-1}$, $2.5 \times 10^{-3}s^{-1}$, and $8.3\times 10^{-4}s^{-1}$). Based on their experiments, one of their conclusions is that the n value (strain hardening exponent) decreases with increasing temperatures but increases with increasing strain rates. As well known in macro scale sheet metal forming, the intercept of forming limit curve at the major strain axis is approximately equal to the strain hardening exponent n. As the increasing of n-value, the forming limit curve will be shifted upward, i.e. the higher n value, the better stretchability. Kwon et al. (2013) conducted a series of tensile tests on Al 1100 foils (96μm) with 1500μm gauge length and 300μm width at six different strain rates ($0.001s^{-1}$, $0.01s^{-1}$, $0.\ 1s^{-1}$, $1s^{-1}$, $10s^{-1}$, and $100s^{-1}$). As discovered in their study, the strain rate had a considerable effect on stress flow, strain hardening, and fracture elongation, which increase with increasing strain rate. This indicates the strain rate has a positive influence on improving the formability of the aluminium foil.

Based on these literatures, strain rate has a positive influence on the formability of the macro sheet forming and foil forming. However, for further understanding the effect of strain rate on improving the formability of CP Ti foils, a series of meso limited dome height (meso-LDH) tests with three different punch speeds (0.01mm/sec, 12m/sec and 17m/sec) were conducted at room temperature to examine the formability of CP Ti Gr2 with thickness of 38μm in this study. The hemisphere punch used for the meso-LDH test was 20mm and a layer of pure gold (≈50nm) was coated on the surface of the as-received foils for creating micro circular grids (Ø50μm). A Photron high speed camera was used to record and compute the punch speeds during deformation process.

2 Experimental Specimens and Experimental Setup

The tempered CP Ti Gr2 foils with 38μm thickness from Arnold Magnetic Technologies in Illinois were used for this study. The as-received foils were blanked into 50.8mm x 50.8mm square blanks first, and then the micro Au circular grids (50μm) were coated on the blanks before being cut into the specific shapes and geometries for experiments. The detail process of creating micro circular grids can be found from Gau et al. (2013). In order to obtain different deformation modes, four different specimen geometries and sizes (40mm, 30mm, 20mm, and 10mm) shown in **Fig. 1**. were designed and tested. The 40mm specimens were used to obtain biaxial tension mode while 30mm specimens for stretching deformation mode. Plain strain and deep drawing modes can be obtained by testing the 20mm and 10mm specimens, respectively. **Fig. 2.** shows a SEM picture showing some micro circular grids on a specimen.

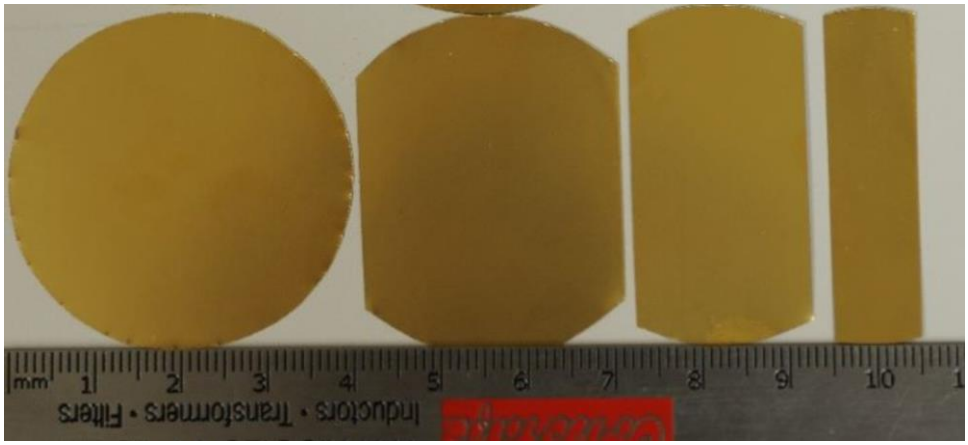

***Figure 1*:** The coating blanks with the Ti foil

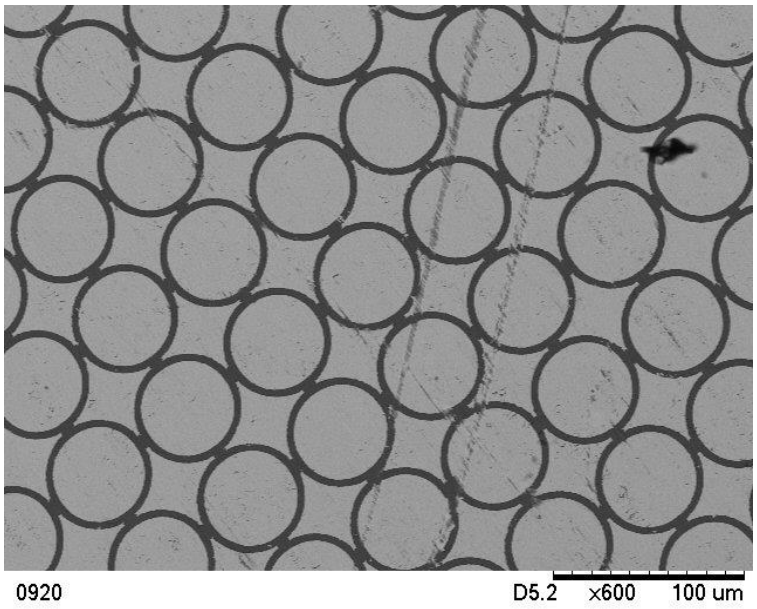

***Figure 2*:** A SEM picture of the micro circular girds (Ø50µm) on a LDH specimen

2.1 Meso-LDH test setup

A series of meso-LDH tests were conducted on a MTS 43 and a pneumatic device for quasi-static speed (0.01mm/sec) and high speed (12m/sec and 17 m/sec) tests, respectively. The setup for the test on MTS 43 is shown in **Fig. 3(a).** while picture (b) shows the hemisphere punch (Ø20mm) for experiments. A pneumatic testing device was designed and built shown in **Fig. 4.** for high speed meso-LDH tests. As shown in picture (c), the devise was mounted on the rail and connected with a gas chamber for experiments. Nitrogen gas was used to fill in the air tank for obtaining any desired pressure. The air released from air tank goes into the pneumatic testing device such that the piston can be accelerated and move the punch to hit and deform the specimen.

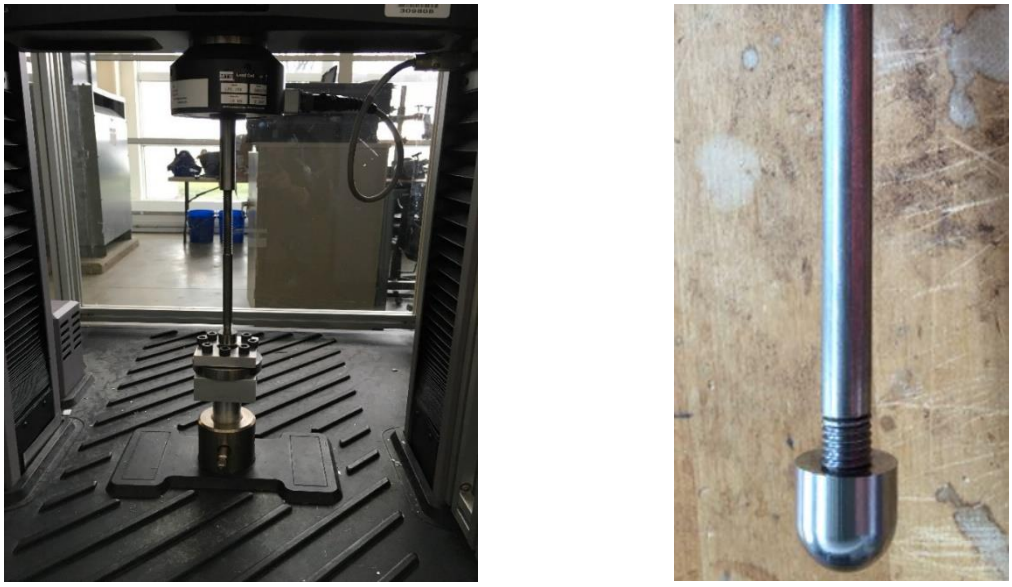

(a) (b)

Figure 3: *(a) The setup for meso-LDH test in MTS 43 (b) Punch used for meso-LDH test*

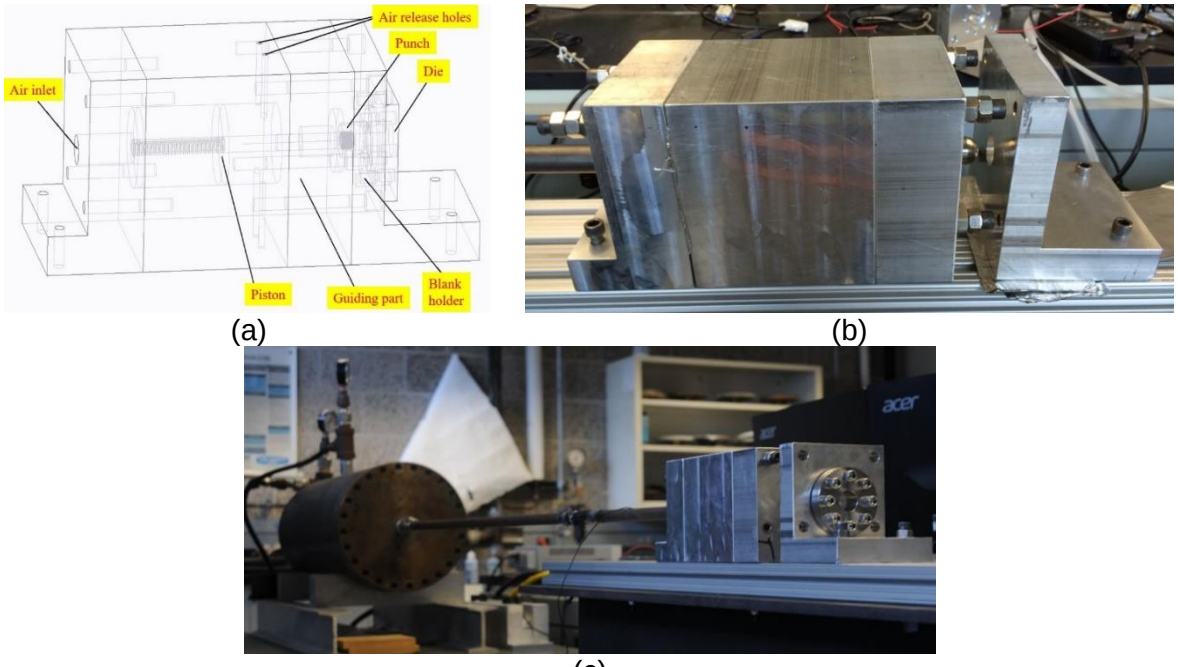

(a) (b)

(c)

Figure 4: *Pneumatic device for high speed meso-LDH test: (a) the sketch of the device, (b) the device, and (c) the setup of the device*

2.2 Conducting Meso-LDH Tests in Quasi-Static Speed

For the quasi-static speed (0.01mm/sec) tests, at least two good specimens for each deformation mode were kept for analysis. The specimens were placed into the blank holder and applied appropriate binding force through adjusting upper binder. The initial position, where the hemispherical punch just touches the surface of the specimen, was found by moving down punch slowly while observing the force change on the MTS 43. In

order to obtain a crack on a specimen as small as possible, the test program can be automatically stopped once the load-displacement curve begins dropping. The smaller crack, the easier to find the initial crack area. **Fig. 5.** shows some specimens tested in 0.01mm/sec punch speed before and after deformations.

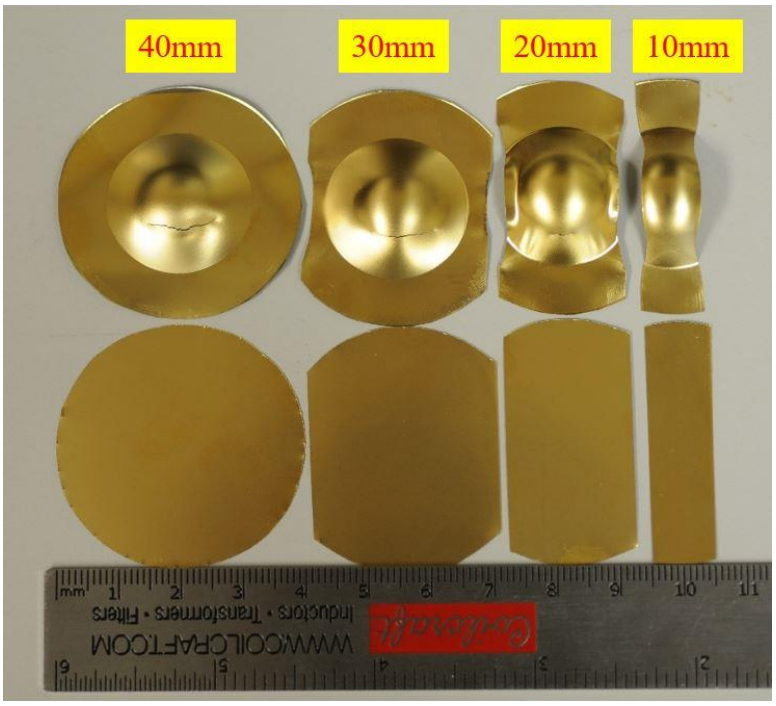

Figure 5: *Meso-LDH test specimens with 20mm punch at 0.01mm/sec speed (before and after test)*

2.3 Conducting Meso-LDH Tests in High

Before conducting meso-LDH tests at high speeds by using the pneumatic device shown in **Fig. 4. ,** it is necessary to know the relation of the pressure in the air tank and punch speed. SO, the process of determining punch speed is as follows. Only two tanks pressures (100psi, 200psi) were used to generate punch speeds in this study. The punch speeds generated by the two pressures were measured by a Photron high speed camera. The high speed camera's recording resolution used in this study were 5000 frames per second and 7500 frames per second for 100pis and 200psi respectively. **Fig. 6.** shows five conterminous frames of 200psi experiments and the 5 pictures shows the spanning location from 6mm to 51mm within which the tests were conducted. Therefore, the average punch speed can be simply computed by $V = {}^{S}/_{t} = \frac{(60-51)/1000}{(\frac{1}{7500}*4)} \approx 17m/sec$. Likewise, the average punch speed at 100 psi was approximate 12m/sec.

Unlike quasi-static speed test, high speed test does not have any signal system showing the occurrence of initial crack so that the test can be automatically stopped. Therefore, in order to get a crack as small as possible, a try and error process was conducted to obtain the optimal dome height by adjusting the axial position of blank holder on the rail shown in **Fig. 4 (c).** The specimen was put into between the blank holder and

the die. The 20mm punch was propelled by nitrogen gas at desired pressure released from air tank to deform the specimen. For each deformation mode, at least two good specimens were kept for data analysis. **Fig. 7.** and **Fig. 8.** show the meso-LDH specimens tested at 12m/sec speed and 17m/sec speed respectively.

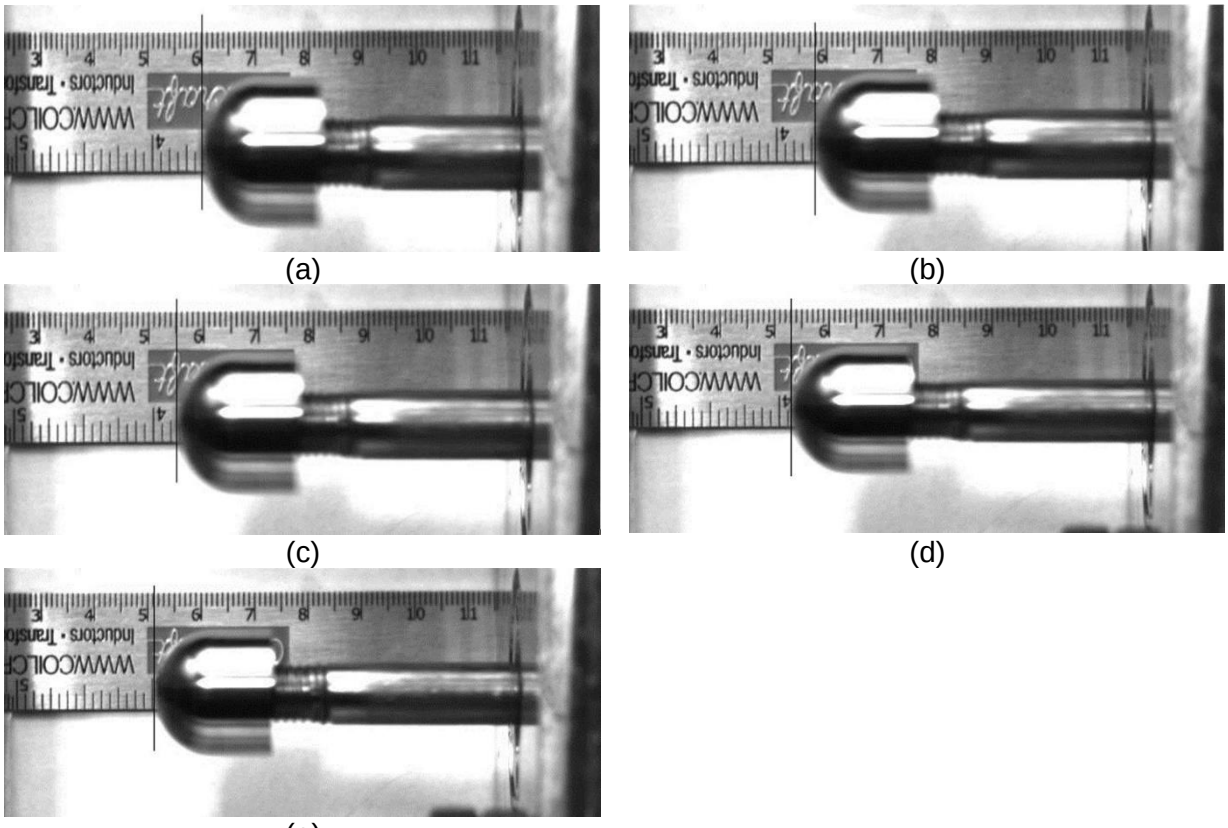

Figure 6: *Five conterminous frames at 200psi*

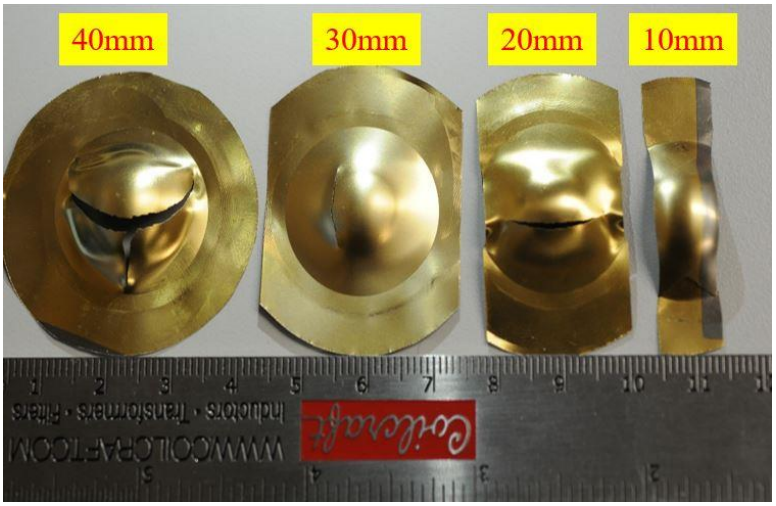

Figure 7: *Meso-LDH test deformed specimens with 20mm punch at 12m/s*

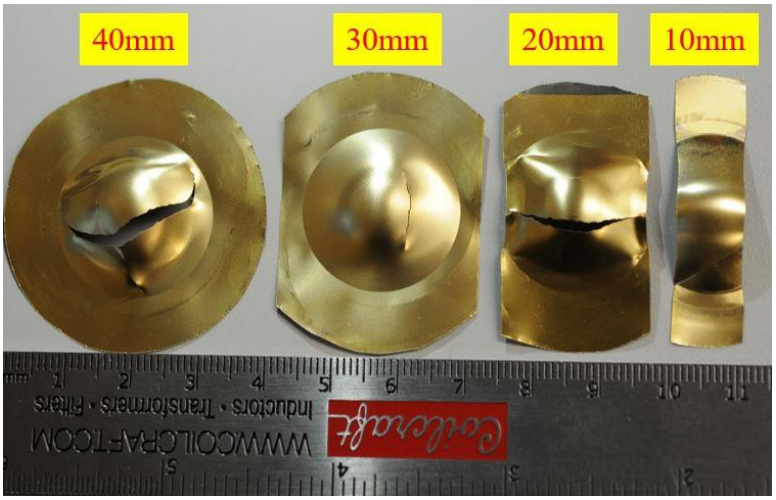

Figure 8: *Meso-LDH test deformed specimens with 20mm punch at 17m/s*

3 Strain Measurement and Constructing FLC

After completing all tests at different test speeds, Scanning electronic microscope (SEM) in NIU clean room was used to take pictures on the area of the initial cracks. ASTM E2218-02 standard (2008) and the method of determining safe and necking grids in the author's prior publication (Gau et al. (2013)) were used to determine the necking and safe grids. **Fig. 9.** shows some pictures of the initial crack areas of meso-LDH test specimens (20mm width blanks) with different punch speeds, on which the micro grids denoted by red number were necking and the black safe. Based on the pictures in **Fig. 9.** only, it can be projected that the higher punch speeds, the better formability. ImageJ, a NIH public domain software, was used to measure the major and minor true strains of the micro circular grids on the pictures taken by the SEM with 250 times magnifications.

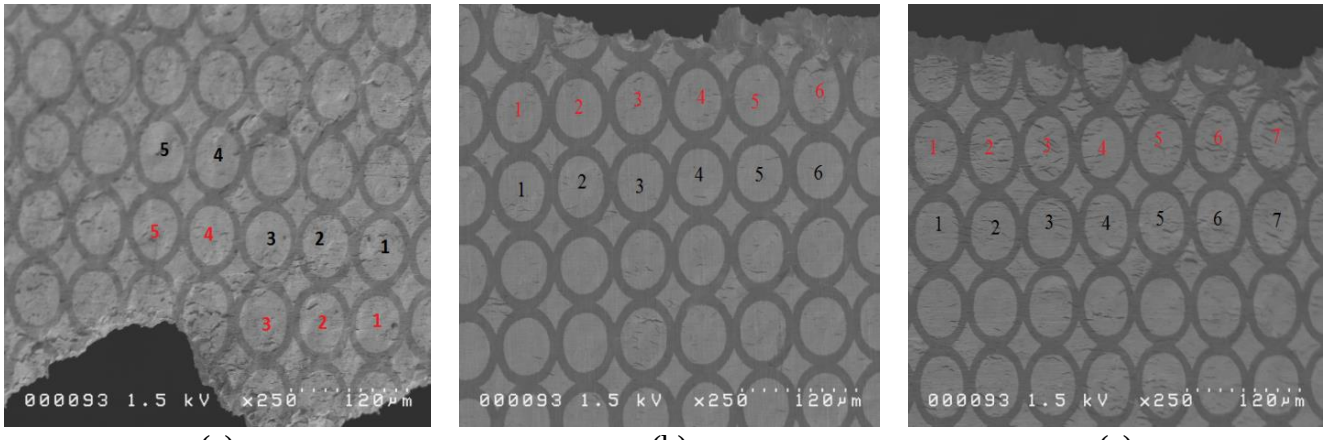

(a) (b) (c)

Figure 9: *SEM pcitures of meso-LDH plan strain specimens tested at different speeds: (a) 0.01mm/sec, (b) 12m/sec, and (c) 17mm/sec*

4 Experimental Results and Discussions

The techniques illustrated in Gau et al. (2013) was used to construct the FLCs of the as-received foils tested at 0.01mm/sec, 12m/sec and 17m/sec, respectively, that are shown in **Fig. 10.**, **Fig. 11.** and **Fig. 12.** The red triangles and blue dots represent the selected necking and safe grids, respectively while black curves are the forming limit curves. Second order polynomial equations for left side curve and right side curve are also shown in the figures.

Fig. 13. shows a comparison of the FLCs of CP Ti Gr2folis tested at three different punch speeds (0.01mm/sec, 12m/sec and 17m/sec). The method of estimating strain rate at laser shock forming of Veenaas and Vollertsen (2016) was used in this study to determine the strain rates of the high speed meso-LDH tests. Table 1 shows the FLC_0 values of the foils tested at different punch speeds (strain rates). The corresponding strain rates of 0.01mm/sec, 12m/sec and 17m/sec punch speeds are ≈0.0005s-1, ≈500s-1, and ≈700s-1, respectively. It can be observed easily from **Fig. 13.** that the effect of strain rate on the formability of CP Ti Gr2 foils is remarkable. In addition, the increment of FLC_0 from quasi-static speed (0.01mm/sec) to punch speed at 12m/sec and 17m/sec are 55.2% and 103.7% respectively. This echoes the research of Tsao et al. (2012) on their comments in increasing strain rate during tensile test. According to their study, the strain hardening coefficient i.e. n-value increases with the increasing of strain rates. As well known, the intercept of forming limit curve at the major strain axis is approximately equal to the strain hardening exponent n. As the increasing of n-value, the forming limit curve will be shifted upward which means better formability.

In addition, the thermal effect and friction are another two important influences of improving formability in this study. As stated in the paper of Talyan et al. (1998), a strain rate of 0.1 s^{-1} may be sufficiently high to introduce a nearly adiabatic condition in the 300-series (stainless steel) specimens. Therefore, the adiabatic effect took place in the high speed meso-LDH tests with 500 s^{-1} and 750 s^{-1} rates in this study. Furthermore, according to the conclusions of experimental study of Kapoor and Nemat-Nasser (1998) on commercially pure Ti and other metal alloys, close to 100% of the plastic work during high strain rate deformation was converted to heat due to adiabatic effect. This resulted in the temperature increased in the deformed specimens due to plastic strain energy and adiabatic effect.

For high speed forming, the deformation is completed in a very short time, normally shorter than 0.001 second, so the generated heat has no time to be dissipated through conduction and convention. For example, the meso-LDH tests conducted at 17m/sec were completed within 0.0006 second. Therefore, the specimens were heated up rapidly by the generated heat due to plastic work and adiabatic effect. The area with higher plastic deformation has higher temperature, so better formability, because thermal effect has a positive influence on the formability of CP Ti Gr2. This is the reason why the FLCs of high speed tests (12 m/sec and 17m/sec) are better than quasi-static one (0.001m/sec).

It is well known that friction has a negative influence on the formability in sheet and foil metal forming. When friction is decreased, FLC can be extended more into stretch mode and even biaxial tension mode. Another advantage of high speed forming can be observed from **Fig. 13.** and the reason is illustrated as follows. As shown in **Fig. 13.**, the right hand side of forming limit curve at quasi-static speed is quite short which means the

stretchability of CP Ti Gr2 foil is lower. However, with the increasing of forming speed, not only does the major strain go higher, but also the minor strain become larger. Therefore, the negative influence of friction can be reduced when the punch speed (strain rate) increases.

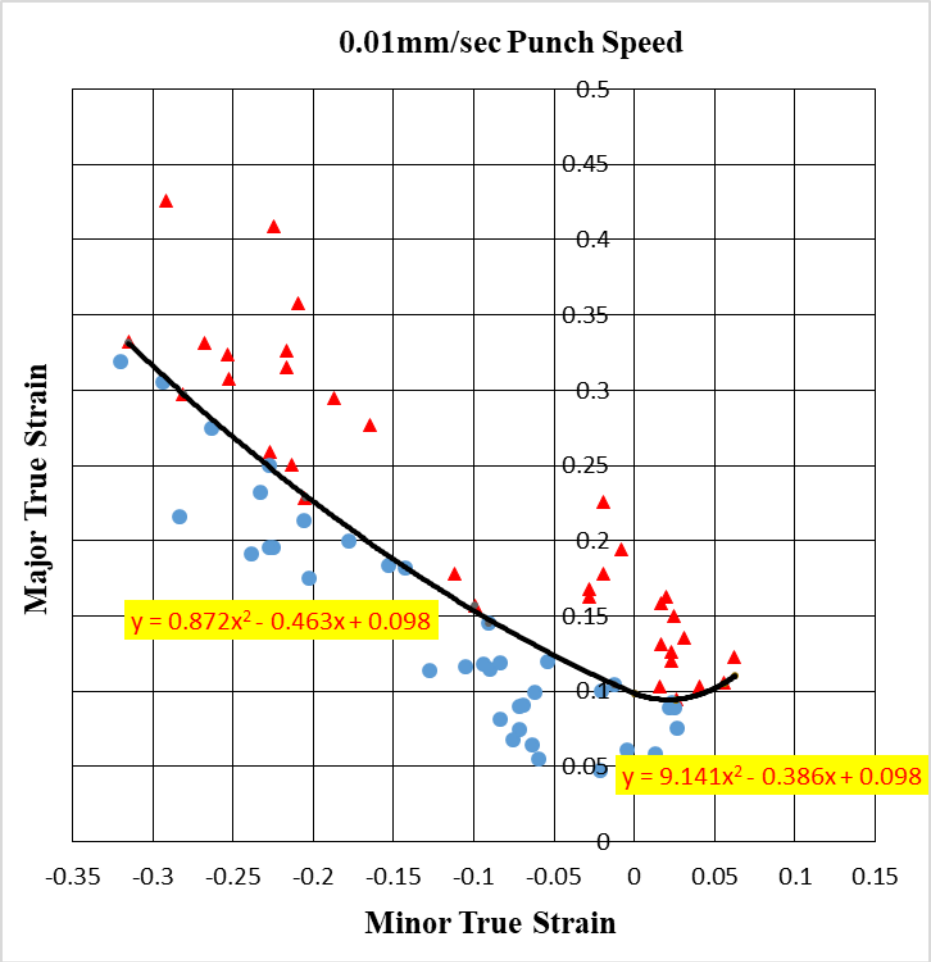

Figure 10: *Forming limit curve of CP Ti Gr2 tested at 0.01mm/sec punch speed*

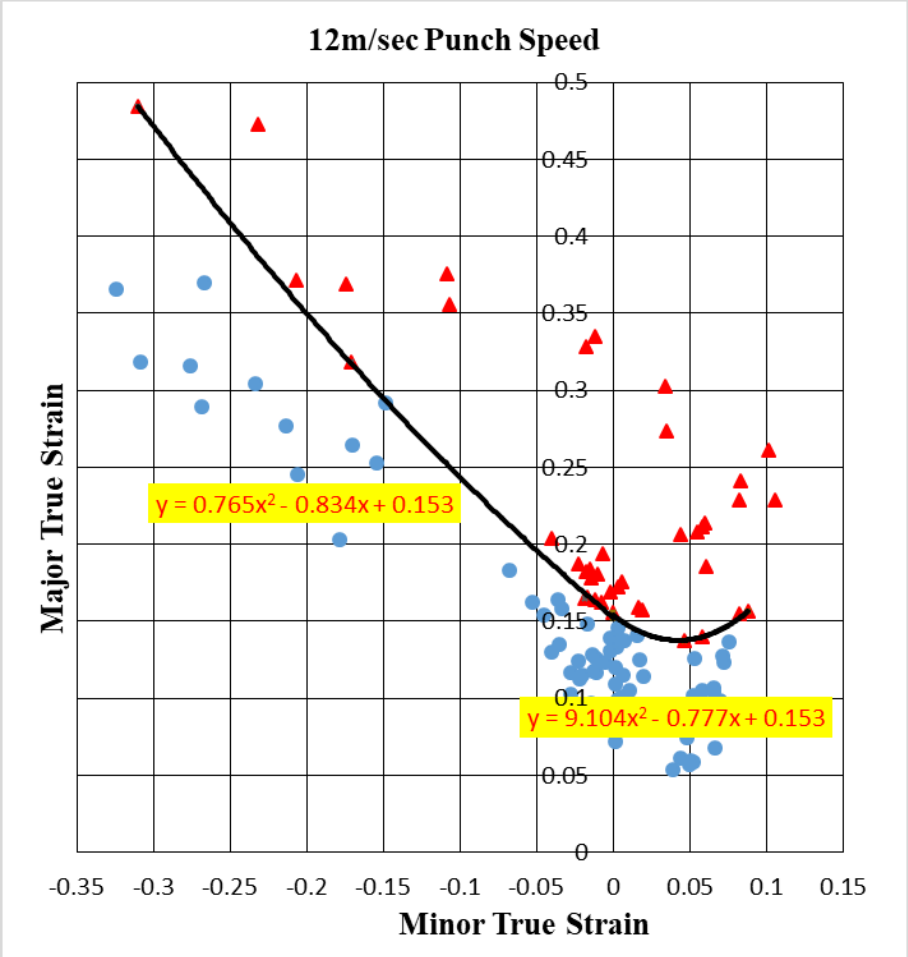

***Figure* 11:** Forming limit curve of CP Ti Gr2 tested at 12m/sec punch speed

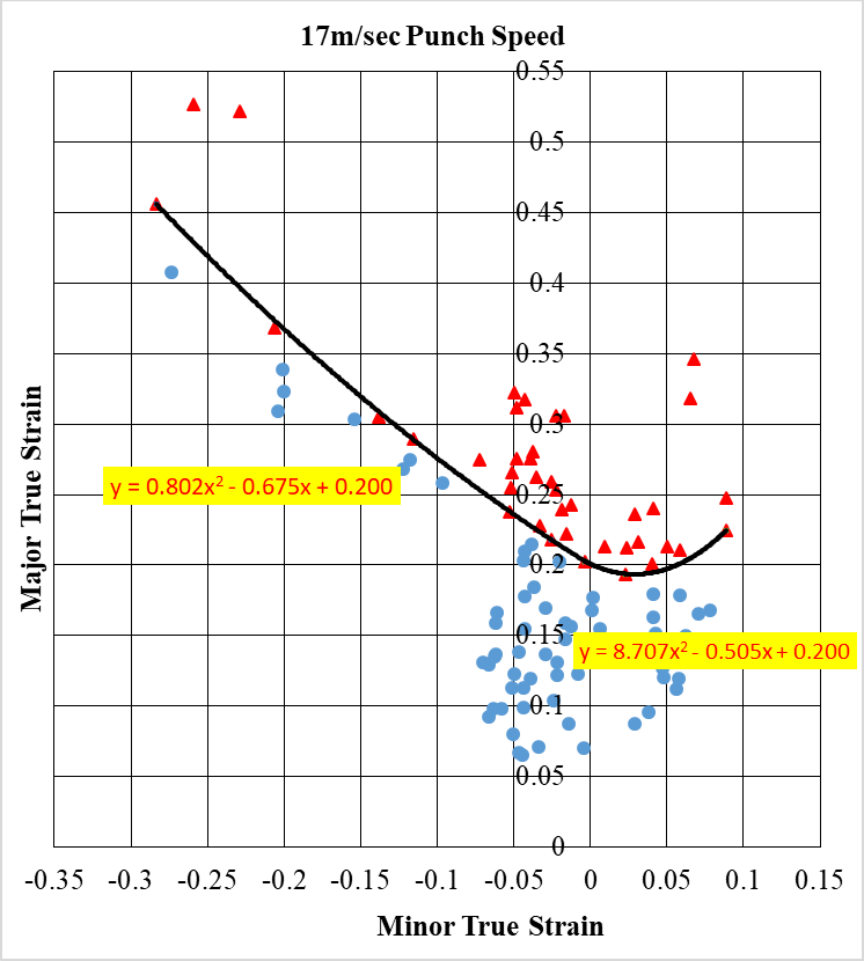

Figure 12: *Forming limit curve of CP Ti Gr2 tested at 17m/sec punch speed*

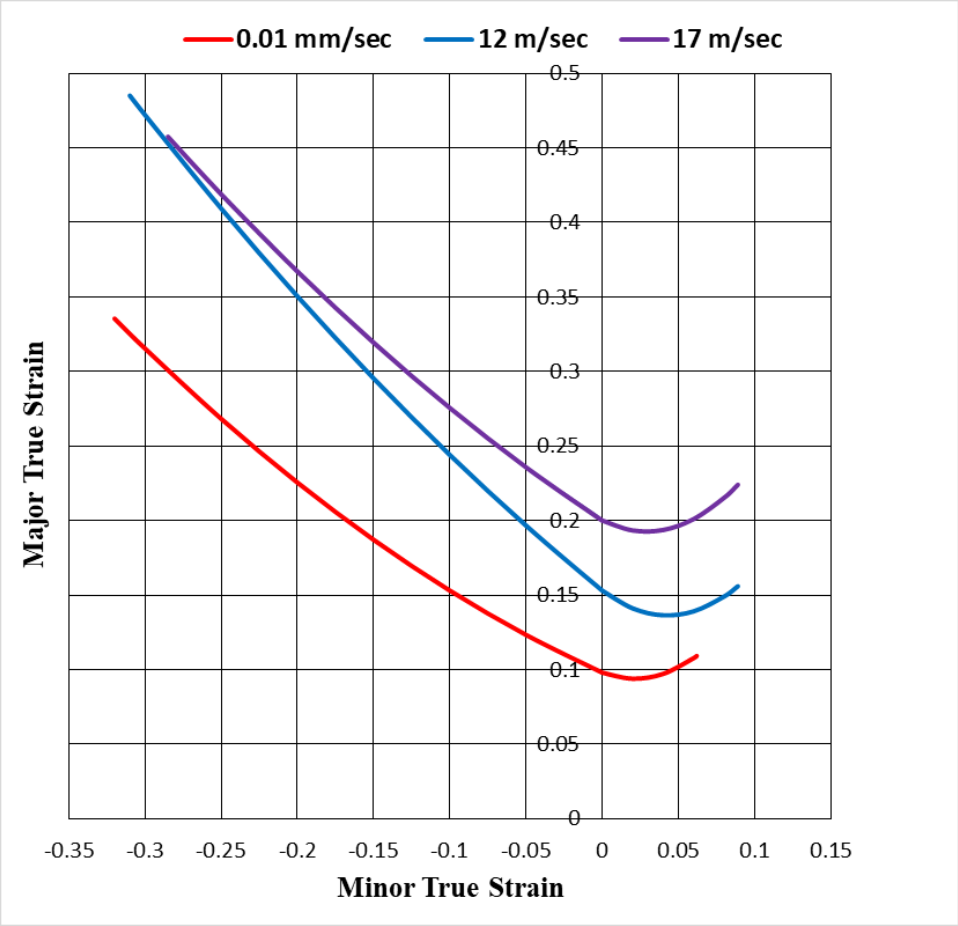

Figure 13: *FLCs with 20mm punch at different speeds*

Table 1
FLC_0 values at different punch speeds

FLC_0			
Punch speed	0.01mm/sec	≈12m/sec	≈17m/sec
Strain rate	≈0.0005s^{-1}	≈500s^{-1}	≈750s^{-1}
	0.098	0.153	0.200

5 Conclusion

In this study, a series of meso-LDH tests were conducted at one quasi-static speed and two high speeds by using a 20mm hemispherical punch to study the effect of strain rates on the formability of CP Ti Gr2 foil (38μm). Three forming limit curves for 3 different strain rates (punch speeds) were obtained, that can be used for industries for die design, process design and simulation, product design, etc. right away. The results of this paper will enhance our abilities to form three dimensional CP Ti Gr2 parts with extremely thin thickness, complex geometry and tight tolerance in high speeds, e.g. the extremely thin fuel cell bipolar plates with micro channels. This will also expand the applications of

commercial pure grade 2 titanium foil through improving its manufacturability at room temperature. Finally, the reasons why the formability of CP Ti Gr2 foils can be improved by increasing strain rate are summarized as below.

1. The n value, an indicator of material stretchability, increases with increasing strain rate (punch speed).
2. The temperature of the deformed part was increased rapidly due to plastic work and adiabatic effect.
3. The negative influence of friction on formability of CP Ti foils can be reduced proportionally with increasing punch speed (strain rate).

References

Arnold Magnetic technologies. 2018. http://www.arnoldmagnetics.com/precision-thin-metals/Materials/Titanium-Its-Alloys

ASTM E2218-02, 2008. Standard test method for determining forming limit curves. ASTM International.

Chen, F.K., Chiu, K.H., 2005. Stamping formability of pure titanium sheets. Journal of Materials Processing Technology. 170(1), 181-186.

Gau, J.T., Chen, P.H., Gu, H., Lee, R.S., 2013. The coupling influence of size effects and strain rates on the formability of austenitic stainless steel 304 foil. Journal of Materials Processing Technology. 213(3), 376-382.

Kapoor, R., Nemat-Nasser, S., 1998. Determination of temperature rise during high strain rate deformation. Mechanics of Materials. 27(1), 1-12.

Kwon, J. B., Huh, J., Huh H., Kim, J. S., 2013. Micro-tensile tests of aluminium thin foil with the variation of strain rate. In Dynamic Behavior of Materials. 1, 89-100.

Tsao, L.C., Wu, H.Y., Leong, J.C., Fang, C.J., 2012. Flow stress behavior of commercial pure titanium sheet during warm tensile deformation. Materials & Design. 34, 179-184.

Talyan, V., Wagoner, R.H., Lee, J.K., 1998. Formability of stainless steel, Metallurgical and Materials Transactions A. 29, 2161-2172.

Veenaas, S., Vollertsen, F., 2016. Determination of strain rate at laser shock forming. Journal for Technology of Plasticity. 41 (2).